Photophysical Properties of $(O_2(^1\Delta_g))_2$ and $O_2(^1\Sigma_g^+)$ in Solution Phase

Pi-Tai Chou,* Youn-Chan Chen, Ching-Yen Wei, Shu-Juan Chen, and Hui-Ling Lu

Department of Chemistry, The National Chung-Cheng University, Chia-Yi, Taiwan, R.O.C.

Tai-Huei Wei

Department of Physics, The National Chung-Cheng University, Chia-Yi, Taiwan, R.O.C.

Received: June 10, 1997[⊗]

Using the C_{60} fluorescence as a reference in combination with the direct spectroscopic observation of $^1O_2$ visible emission, the photophysics of $^1O_2$ dimol ($(^1\Delta_g)_2$) and $O_2(^1\Sigma_g^+)$ states in solution has been studied. The quantum yield of O_2 $^1\Sigma_g^+ \rightarrow {}^3\Sigma_g^-$ (765 nm) emission has been measured to be 1.94×10^{-7}, and consequently, the radiative decay rate of $^1\Sigma_g^+ \rightarrow {}^3\Sigma_g^-$ transition was determined to be 1.55 ± 0.04 s^{-1} which, within the experimental error, is consistent with the previous report of 0.46 s^{-1}.[4] Further determination of the ratio between radiative decay and dissociation rates of the $^1\Delta_g$ dimol has been achieved by comparing the dimol $(^1\Delta_g)_2 \rightarrow (^3\Sigma_g^-)_2$ emission intensity with the tetra-*tert*-butylphthalocyanine delayed fluorescence induced by a two-step energy transfer from the $O_2(^1\Delta_g)$ state. As a result, the lower limit of the dissociation rate constant of the dimol was estimated to be $(2.6 \pm 0.3) \times 10^{10}$ s^{-1} in CCl_4.

Introduction

Only recently has the investigation of singlet oxygen visible emission in solution phase become possible with the detection of O_2 $^1\Sigma_g^+ \rightarrow {}^3\Sigma_g^-$ 765 nm and O_2 dimol $(^1\Delta_g)_2 \rightarrow (^3\Sigma_g^-)_2$ 634 and 703 nm vibronic peaks.[1−6] Using an interference filter to isolate the emission at 765 ±19 nm coupled with a red-sensitive photomultiplier, Schmidt and Bodesheim[1−4] were capable of extracting a portion of the decay attributed to the $^1\Sigma_g^+$ decay. Consequently, photophysical properties of the $^1\Sigma_g^+$ state in solution have been studied.[2] On the other hand, Krasnovsky and Foote[5] applied an indirect time-resolved method which incorporates $O_2(^1\Delta_g)$ dimol sensitizing tetra-*tert*-butylphthalocyanine (PC) luminescence to study the relaxation dynamics of the $O_2(^1\Delta_g)$ dimol. However, evidence against dimol-sensitized PC luminescence in solution has recently been reported by Gorman et al.[6] Their data are only consistent with a two-step mechanism which involves the $^1\Delta_g$ sensitizing PC to its triplet state (i.e., ^{3}PC) followed by the second-step energy transfer from$^1\Delta_g$, producing the excited singlet PC. More recently, using an ultrasensitive intensified charge-coupled detector we have simultaneously observed photosensitized O_2-$(^1\Delta_g)$ dimol and $O_2(^1\Sigma_g^+ \rightarrow {}^3\Sigma_g^-)$ emission spectra in solution.[7] Taking advantage of direct spectroscopic observation, studies of photophysical properties such as quantum yield, radiative lifetime, etc. for these ultraweak $^1O_2$ forbidden transitions, especially the $^1O_2$ dimol in solution phase, may become feasible.

In order to achieve these goals, the first step of this seminal study is to select a suitable compound as a reference for the quantum yield measurement. Organic dyes such as quinine sulfate, anthracene, etc. commonly used as references for relative quantum yield measurements usually have fluorescence yields >0.1. Therefore, significant error may be introduced when comparing such a strong emission with the ultraweak $^1O_2$ emission ($\Phi < 10^{-5}$, vide infra) in the visible region. Furthermore, the emission wavelengths of these dyes are generally in the region of <700 nm which are too far away from the studied $^1O_2$ spectrum to have a fair comparison, especially when the response of the detecting system is significantly wavelength-dependent. Numerous results have revealed that C_{60} should be a good fluorescence reference for such an application. C_{60} exhibits a very weak fluorescence maximum at ∼700 nm in various solvents, which coincidentally overlaps with $^1O_2(^1\Sigma_g^+)$ and $^1O_2$ dimol vibronic peaks. The fluorescence quantum yields of 2.0×10^{-4} and 2.2×10^{-4} for C_{60} have been accurately determined in neat *n*-hexane and toluene, respectively.[8,9] More importantly, it was found that fluorescence spectra and fluorescence quantum yields of C_{60} are excitation-wavelength independent for different bands of the absorption spectrum.[9] These, in combination with its high photostability toward laser irradiation, make C_{60} a suitable reference compound to determine the quantum yield of the ultraweak $^1O_2$ emission in the visible region.

The following sections are organized according to a sequence of steps where we first attempt to use the C_{60} fluorescence as a reference to determine relative quantum yield and radiative lifetime of the O_2 $^1\Sigma_g^+ \rightarrow {}^3\Sigma^-_g$ (765 nm) emission. The result was consistent with the previous report based on a time-resolved measurement, indicating that the direct spectral measurement is not only valid but also a simpler approach. The next step involved a series of experiments and kinetic derivations to determine the photophysical properties of the $O_2(^1\Delta_g)$ dimol. This has been achieved mainly by comparing the directly sensitized $^1O_2$ dimol 634 and 703 nm emission intensity with respect to the PC delayed fluorescence sensitized by two-step energy transfer from $O_2(^1\Delta_g)$. Consequently, the ratio of radiative decay and dissociation rates for the $(^1\Delta_g)$ dimol can be extracted. The result leads to a reasonable estimation of the dissociation rate of the $^1O_2$ dimol. Finally, detailed relaxation pathways of the $^1O_2$ dimol and the triplet-state energy level of C_{60} will be discussed.

Experimental Section

Material. PC was synthesized according to the previously reported method.[10] The final product was purified by column chromatography (eluent $CHCl_3$), and the spectral purity of PC

* To whom the correspondence should be addressed.

⊗ Abstract published in *Advance ACS Abstracts,* October 15, 1997.

S1089-5639(97)01886-0 CCC: $14.00

was checked by the fluorescence excitation spectrum. 1*H*-phenalen-1-one (PH, Aldrich) was purified by column chromatography (*n*-hexane:ethyl acetate 1:1 v/v) followed by twice recrystallization from methanol. C_{60} was purified by chromatography on neutral alumina according to a previous report.[11] CCl_4 was dried by passing through Al_2O_3 followed by refluxing for several hours. The dry CCl_4 was then obtained through fractional distillation under N_2 atmosphere. Since the entire purification process was under nitrogen, it was necessary to purge the dry solution with oxygen to prepare various oxygen concentration. The molar ratio of oxygen in solution was determined by Henry's law from a known O_2 concentration at 760 Torr for various solvents.[12] Toluene (BDH) was used as received because no interference of the impurity fluorescence was detected in the wavelength region of interest.

Measurement. In steady-state experiments, an Ar^+ laser (Coherent, Innova 90, 6 W) tuned to either 350 or 514 nm was used as an excitation source, while in the time-resolved study either the second (532 nm) or third (355 nm) harmonic of a Nd:YAG laser (Continuum, Surlite II) was applied. The spectral detection in the region of 600−800 nm was accomplished by a red-sensitive intensified charge coupled detector (ICCD, Princeton Instrument, Model 576G/1) coupled with a polychromator in which the grating is blazed with a maximum at 700 nm. Two different methods were applied for the spectral detection in the near-IR region. In the region of 1000−1700 nm a liquid nitrogen cooled, slow response-time (∼10 ms) Ge photodiode (Applied Detector Corp. Model 403L) coupled with an SRS (Stanford Research System Model SR830) lock-in amplifier was used for steady-state measurements. Details of the setup have been elaborately described elsewhere.[13,14] In the region of 1700−2500 nm we applied a Fourier transform technique in which the emission was collected by a camera lens (Nikon, $f =$ 1.2), sent through a near-IR interferometer (Bruker Equinox 55) and detected by a liquid nitrogen cooled InAs detector (Judson Infrared Model J12-D) equipped with a Judson Model 700 amplifier. A series of holographic filters (Kaiser Optical Systems, Inc.) were used to exclude the 355, 514, and 532 nm excitation laser wavelengths. For the 350 nm Ar^+ excitation, the scattering laser light was eliminated by a Scott GG-495 filter which has constant transmittance (95%) in the region of >600 nm.

The time-resolved measurement for the long-lived $^1\Delta_g$ 1273 nm emission in CCl_4 was achieved by using a chopped (10.0 Hz) CW Ar^+ excitation which produced a ∼2.0 ms duration pulse. A similar setup using a chopped CW Ar^+ light source to measure the long-lived $^1\Delta_g$ 1273 nm emission in halogenated solvents has been reported by Schmidt and Brauer.[15] The output impedance of the preamplifier has been modified so that the response time of the aforementioned Ge detector was reduced to 1.2 ms. The lifetime of the PC fluorescence was measured by an Edinburgh FL 900 photon counting system for which the data acquisition and analysis have been elaborately described.[16]

For the direct measurement of $^1O_2$ visible emission, PH or C_{60} was used as a sensitizer of which the same optical density of 3.0 was prepared at 350 nm. Taking ϵ_{350} of 9550 and 33 270 L mol^{-1} cm^{-1} in CCl_4, the concentration of PH and C_{60} is calculated to be 3.14×10^{-4} and 9.0×10^{-5} M, respectively. For the $O_2(^1\Delta_g)$ sensitizing PC experiment, C_{60} was used as a photosensitizer to generate $O_2(^1\Delta_g)$. Due to the limiting solubility of C_{60} and low absorptivity at 514 nm ($\epsilon = 910$ L mol^{-1} cm^{-1} in CCl_4), an optical density of 0.5 was prepared at 514 nm, corresponding to a concentration of C_{60} of 5.5×10^{-4} M. PC was prepared in the absorbance range of 0.2−2.0 at 700 nm, corresponding to a concentration in the range of 1.25×10^{-6} to 1.25×10^{-5} M ($\epsilon_{700} = 1.60 \times 10^5$ L mol^{-1} cm^{-1} in CCl_4). Under such concentrations, the optical density of PC is between 2.0×10^{-3} and 2.0×10^{-2} at 514 nm. Therefore, the PC fluorescence interference resulting from the direct 514 nm excitation is very small and can be subtracted from the sensitized PC fluorescence (vide infra). The sample cuvette was excited at the edge of the fluorescence cell to avoid the inner filter effect.

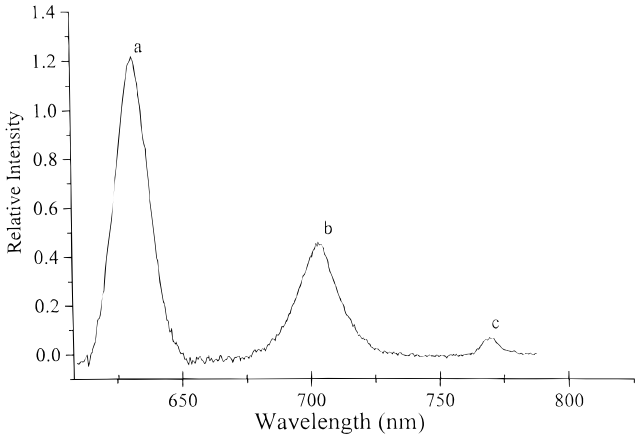

Figure 1. Emission spectra of O_2 (2.48×10^{-3} M) sensitized by PH in CCl_4 at 25 °C; peaks a and b correspond to the $O_2(^1\Delta_g)$ dimol $(^1\Delta_g)_2 \rightarrow (^3\Sigma_g^-)_2$ transition and peak c to the $^1\Sigma_g^+ \rightarrow {}^3\Sigma_g^-$ emission. The PH (3.14×10^{-4} M) was excited by a CW Ar^+ laser (350 nm, 50 mW with a beam diameter of ∼2.0 mm).

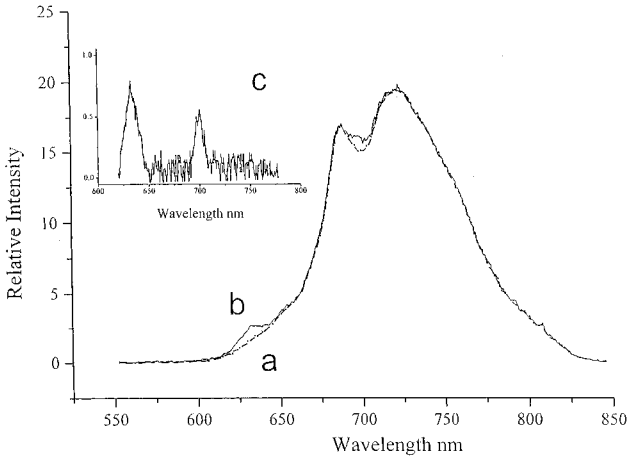

Figure 2. Emission spectra of C_{60} (9.0×10^{-5} M) in a (- - -) aerated and b (—) deaerated CCl_4. Inset c shows the emission spectrum obtained by subtracting spectrum a from spectrum b. Except for different sensitizers, the experimental conditions were the same as that of Figure 1.

Results and Discussion

Figure 1 shows the non-time-resolved PH sensitized $^1O_2$ visible emission spectra in the region of 600−800 nm after subtracting the baseline resulting from the phosphorescence of PH. Three vibronic emission maxima at 634, 703, and 765 nm were resolved, which have been unambiguously assigned to $^1O_2$ dimol ($(^1\Delta_g)_2(0,0) \rightarrow (^3\Sigma_g^-)_2(0,0)$ and $(^1\Delta_g)_2(0,0) \rightarrow (^3\Sigma_g^-)_2(0,1)$) emission and $O_2(^1\Sigma_g^+(0) \rightarrow {}^3\Sigma_g^-(0))$ emission,[7] respectively. Figure 2a shows the fluorescence spectrum of C_{60} in the oxygen-free CCl_4 solution, which consists of two major vibronic peaks with maxima at 685 and 720 nm. The spectral features are very similar to the fluorescence of C_{60} in toluene[9] except that the emission maximum is blue-shifted by ∼5 nm possibly due to the solvent polarization effect. Figure 2b shows the fluorescence spectrum of C_{60} in the oxygenated CCl_4 solution

under similar experimental conditions as that used to obtain Figure 2a. In addition to a similar fluorescence spectrum for C_{60} with respect to the oxygen-free spectrum in Figure 2a, a new emission band appears with a peak maximum at ~634 nm. Since the spectral feature resembles that of the 634 nm emission shown in Figure 1, and this emission vanishes upon degassing (see Figure 2a), its assignment to the $^1O_2$ dimol $(^1\Delta_g)_2(0,0) \rightarrow (^3\Sigma_g^-)_2(0,0)$ emission is unambiguous. The 703 nm $(^1\Delta_g)_2(0,0) \rightarrow (^3\Sigma_g^-)_2(0,1)$ vibronic emission is hidden inside the major peaks of the C_{60} fluorescence. Since the fluorescence intensity of C_{60} is nearly independent of the O_2 concentration due to the ultrashort lifetime, several 10 ps,[9,17−19] of C_{60} fluorescence, the 703 nm peak can be resolved by subtracting Figure 2a from Figure 2b after normalization, and the result is shown in the inset of Figure 2 (Figure 2c). Interestingly, although the 634 and 703 nm vibronic peaks resulting from $^1O_2$ dimol were resolved, within the detection limit of our system, the 765 nm $^1\Sigma_g^+ \rightarrow {}^3\Sigma_g^-$ emission was not observed (vide infra).

Since Figures 1 and 2 were obtained under an experimental condition so that the number of photons being absorbed by the sensitizers are identical, the information allows us to perform a steady-state quantum yield measurement for the $^1O_2$ visible emission. For the first attempt, the relative quantum yield of the $^1\Sigma_g^+$ state in CCl_4 with respect to that of C_{60} in toluene was calculated on the basis of the following relationship

$$\frac{\Phi(^1\Sigma_g^+)_{CCl4}}{\Phi(C_{60})_{C_6H_8}} = \frac{\int n_{CCl_4}{}^2 F\Sigma_g^+(\tilde{\nu})\, d\nu}{\int n_{C_6H_8}{}^2 F_{C_{60}}(\tilde{\nu})\, d\nu}$$

where $F^1\Sigma_g^+(\tilde{\nu})$ and $F_{C_{60}}(\tilde{\nu})$ are the corrected fluorescence spectra of $^1\Sigma_g^+$ and C_{60}, respectively. n denotes the index of refraction of the solvent, which is 1.496 for toluene and 1.594 for CCl_4.[20] The integrated 765 nm emission intensity (Figure 1) is only 5.5×10^{-4} of the overall C_{60} fluorescence intensity. Taking $\Phi(C_{60})_{C_6H_8}$ to be 2.2×10^{-4},[9] the quantum yield of $^1\Sigma_g^+$ was calculated to be 1.2×10^{-7}. However, this value is obtained under the circumstance that the production of the $^1\Sigma_g^+$ state is 100% upon sensitization. Since PH has been reported to produce $^1\Sigma_g^+$ in a yield of only 0.62,[2] the quantum efficiency of the $^1\Sigma_g^+ \rightarrow {}^3\Sigma_g^-$ emission was further corrected to be 1.94×10^{-7}. Taking the average decay rate of the $^1\Sigma_g^+$ state to be 122 ± 5 ns by time-resolved spectral evolution[7] and 130 ± 10 ns by the transient lifetime measurement,[3] the radiative decay of $^1\Sigma_g^+ \rightarrow {}^3\Sigma_g^-$ emission, k_r, according to $k_r = k_{obs}\Phi(^1\Sigma_g^+)$, was calculated to be 1.55 ± 0.04 s^{-1}. On the basis of integrating the time-resolved $^1\Sigma_g^+$ 765 nm decay in comparison with the integrated decay of tetraphenylporphine (TPP) emission, Schmidt and Bodsheim[4] have calculated the quantum yield of $^1\Sigma_g^+ \rightarrow {}^3\Sigma_g^-$ emission to be 5.8×10^{-8}. Consequently, a radiative decay rate of 0.45 s^{-1} was deduced. In comparison, our values are 3 times as fast. This discrepancy is believed to result from different experimental conditions, namely steady-state versus time-resolved measurements. One possibility is that the intensity as well as lifetime of TPP is pulse energy dependent. As a result, the quantum yield of TPP measured by the time-resolved method may be different from that of the steady-state approach. Nevertheless, our result is comparable with the time-resolved measurement, but involved a simpler approach. This makes the photophysical studies of the $^1O_2$ dimol, the main goal of this study, feasible.

Since the $^1O_2$ dimol is formed based on a collisional interaction between two $^1O_2$ molecules, its relaxation mechanism involves formation, dissociation and other decay pathways depicted in Scheme 1.

SCHEME 1

$$\text{Sen} \xrightarrow{h\nu} \xrightarrow[(>10^{10}\ \text{s}^{-1})]{\text{intersystem crossing}} \text{Sen(T)}$$

$$\text{Sen(T)} + O_2(^3\Sigma_g^-) \xrightarrow{k_c} \text{Sen}(S_0) + O_2(^1\Sigma_g^+)$$

$$O_2(^1\Sigma_g^+) \xrightarrow{k_s} O_2(^1\Delta_g) \text{ or } O_2(^3\Sigma_g^-)$$

$$O_2(^1\Delta_g) \xrightarrow{k_p} O_2(^3\Sigma_g^-)$$

$$O_2(^1\Delta_g) + O_2(^1\Delta_g) \underset{k_{-ac}}{\overset{k_{ac}}{\rightleftharpoons}} (O_2(^1\Delta_g))_2$$

$$(O_2(^1\Delta_g))_2 \xrightarrow{k_{d1}} (O_2(^3\Sigma_g^-))_2$$

$$(O_2(^1\Delta_g))_2 \xrightarrow{k_{d_2}} O_2(^3\Sigma_g^-) + O_2(^1\Sigma_g^+)$$

where Sen denotes the sensitizer used to generate singlet molecular oxygen. To solve the time-dependent $^1O_2$ dimol concentration we assume that due to the extremely weak $^1O_2-{}^1O_2$ interaction the dissociation rate k_{-ac} of $(^1\Delta_g)_2$ back to two $^1\Delta_g$ species must be very rapid so that k_{-ac} is $\gg k_{ac}[^1\Delta_g]$ and/or k_d $(=k_{d1} + k_{d2})$, the rate of formation and decay of $(^1\Delta_g)_2$, respectively, during the entire life span of $^1\Delta_g$. This viewpoint will also be verified experimentally in a later section after deducing the value of k_{-ac}. Consequently, the time-dependent dimol concentration can be derived by a steady-state approximation for the dimol concentration and the result is shown in eq 1

$$[(^1\Delta_g)_2] = \frac{k_{ac}}{2k_{-ac}}[^1\Delta_g]_0^2 e^{-2k_p t} \qquad (1)$$

where $[^1\Delta_g]_0$ is the initial population of $^1\Delta_g$. Since the radiative decay rate for both PH[21] and C_{60}[9,17−19] in the S_1 state is more than 2 orders of magnitude slower than the rate of intersystem crossing, >99% of the initially excited sensitizer will relax to the triplet state. Furthermore, the yield of $^1\Delta_g$ sensitized by PH has been reported to be near unity (≥ 0.97[21]) in the oxygen-saturated CCl_4 solution. Therefore, $[^1\Delta_g]_0$ is nearly equivalent to the number of photons being absorbed, i.e., number of sensitizers being excited initially when PH was used as a sensitizer. It should be noted that a branching ratio 0.62:0.37 for the production of $^1\Sigma_g^+$ versus $^1\Delta_g$ has been reported by Schmidt and Bodesheim.[4] Their results also conclude that the efficiency of $^1\Sigma_g^+ \rightarrow {}^1\Delta_g$ relaxation is near unity. Since the depletion of the $^1\Sigma_g^+$ state takes place within a few hundred nanoseconds,[4,7] which is much shorter than the relaxation time scale of $^1\Delta_g$ in CCl_4,[22−25] the initial population of $^1\Delta_g$, $[^1\Delta_g]_0$, shown in eq 1 actually results from two pathways: the direct sensitization process from the $(\text{Sen(T)}-{}^3O_2)$ collisional complex and the $^1\Sigma_g^+ \rightarrow {}^1\Delta_g$ relaxation. On the other hand, for the case of using C_{60} as a $^1O_2$ sensitizer the yield of $^1\Delta_g$ is concluded to be 0.85. This value was obtained by monitoring the intensity of the $^1\Delta_g \rightarrow {}^3\Sigma_g^-(0,0)$ 1273 nm emission sensitized by C_{60} with respect to that sensitized by PH, assuming that the yield of $^1\Sigma_g^+ \rightarrow {}^1\Delta_g$ relaxation is near unity.

According to eq 1, the time-dependent dimol concentration reflects the slow and limiting annihilation of two $^1\Delta_g$ molecules,

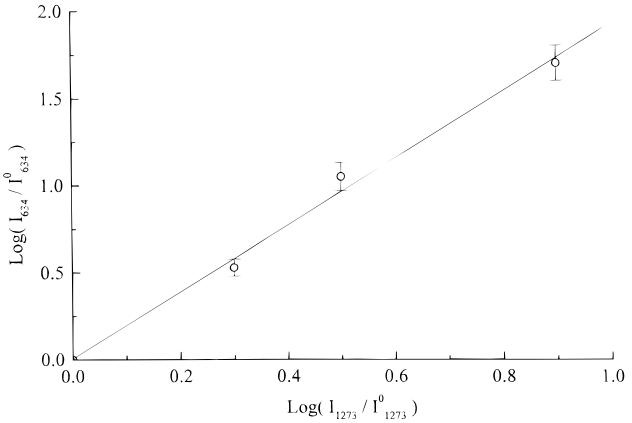

Figure 3. Double logarithmic plot for the $(^1\Delta_g)_2(0,0) \rightarrow (^3\Sigma_g^-)_2(0,0)$ 634 nm emission intensity versus the $^1\Delta_g(0) \rightarrow {}^3\Sigma_g^-(0)$ 1273 nm emission intensity. The superscript zero denotes the emission intensities at the lowest laser power used, which is 20 mW (350 nm) in this study.

which actually corresponds to twice the decay rate of the $^1\Delta_g$ species. For the case of using PH as a sensitizer, the dimol emission response function $I_D(t)$, defined as the quantum intensity of the dimol emission at a time t divided by the number of photons being absorbed, N_0, can be deduced from (1) and expressed in (2).

$$I_D(t) = \frac{k_D[(^1\Delta_g)_2]}{N_0} \sim \frac{k_D[(^1\Delta_g)_2]}{[^1\Delta_g]_0} = \frac{k_D k_{ac}}{2k_{-ac}}[^1\Delta_g]_0 e^{-2k_p t} \quad (2)$$

For the case of using C_{60} as a sensitizer, N_0 should be replaced by $1.18[^1\Delta_g]_0$ due to its 85% $^1\Delta_g$ production. The measured steady-state $(O_2(^1\Delta_g))_2$ emission intensity, F_D, should be proportional to the integrated form of (2) and $[^1\Delta_g]_0$, namely

$$F_D = \alpha \frac{k_D k_{ac}}{4k_p k_{-ac}}[^1\Delta_g]_0^2 \quad (3)$$

where α is the instrument factor, including sensitivity, alignment, etc. of the detecting system. Equation 3 simply indicates that the dimol emission intensity is dependent on the square of $[^1\Delta_g]$, i.e., quadratically proportional to the excitation energy. This should be the case since the dimol formation results from a bimolecular process involving two $^1\Delta_g$ species. Experimentally, this viewpoint can be supported by plotting the logarithm of 634 nm dimol emission intensity versus the 1273 nm $^1\Delta_g \rightarrow {}^3\Sigma_g^-$ emission (see Figure 3), in which a slope of 1.90 was obtained, indicating that the intensity of 634 nm emission band is proportional to the square of the $^1\Delta_g$ concentration. In the time-resolved measurement, $[^1\Delta_g]_0$ in eq 2 is equivalent to the initial population of the triplet state of PH, which may be obtainable by performing a triplet−triplet transient absorption measurement. However, this method introduces significant error due to the inaccuracy in measuring the absolute absorption extinction coefficient of the triplet−triplet transition and the uncertain overlap efficiency between pump and probe pulses. Moreover, disregarding the excitation energy, attempts to resolve the dimol emission based on a nanosecond pulse excitation experiment always results in a very small S/N ratio, which makes the determination of the dimol emission yield relative to that of C_{60} very difficult. This perplexing result may be rationalized by the fact that in CCl_4, the decay rate of $^1\Delta_g$, k_p, increases drastically upon increasing the pulse energy,[22−25] resulting in a decrease of the dimol emission intensity. To overcome this obstacle we have attempted to eliminate the concentration factor in eq 3 by a steady-state approach. This method was accomplished by comparing the dimol emission intensity with respect to the PC delayed fluorescence induced by a two-step $^1\Delta_g$ sensitization mechanism depicted in Scheme 2.

SCHEME 2

$$PC(S_0) + O_2(^1\Delta_g) \xrightarrow{k_q} PC(S_0) + O_2(^3\Sigma_g^-)$$

$$PC(S_0) + O_2(^1\Delta_g) \underset{k_2}{\overset{k_1}{\rightleftharpoons}} PC(T_1) + O_2(^3\Sigma_g^-)$$

$$PC(T_1) + O_2(^1\Delta_g) \xrightarrow{k_3} PC(S_1) + O_2(^3\Sigma_g^-)$$

$$PC(T_1) \xrightarrow{k_4} PC(S_0)$$

$$PC(S_1) \xrightarrow{k_{pc}} PC(S_0)$$

The $^1\Delta_g$ sensitizing PC delayed fluorescence based on the mechanism shown in Scheme 2 has originally proposed by Ogryzlo and Pearson[26] and recently been verified by Gorman et al.[6] According to Scheme 2, the decay dynamics of PC*, i.e., the delayed PC fluorescence, sensitized by $^1O_2$ dimol can be derived by steady-state approaches on $PC(T_1)$ and $PC(S_1)$ and its time-dependent decay dynamics can be depicted in eq 4, where k_{pc} is the decay rate of the prompt (i.e., directly excited)

$$PC^*(t) = \frac{k_1 k_3 [pc][^1\Delta_g]_0^2}{k_2 k_{pc}[^3\Sigma_g^-]} e^{-2(k_p + k_q[PC])t} \quad (4)$$

PC fluorescence. $k_p + k_q[PC]$ is the decay rate of $^1\Delta_g$ when PC is added to the solution, leading to a quenching rate of k_q-[PC]. Equation 4 indicates that the observed decay rate of the PC delayed fluorescence, similar to the $^1O_2$ dimol emission, is also twice as much as the decay rate of the $^1\Delta_g$ emission. In addition, the intensity of the PC delayed fluorescence should be quadratically and inversely proportional to the excitation energy and the $O_2(^3\Sigma_g^-)$ concentration, respectively. These viewpoints have been supported experimentally by Gorman et al.[6] On the contrary, if the PC delayed fluorescence, as proposed by Krasnovsky and Foote,[5] results from the $^1O_2$ dimol sensitization, the sensitized PC emission intensity should be independent of the $O_2(^3\Sigma_g^-)$ concentration. We have also performed an O_2 concentration-dependent study of the PC delayed fluorescence and found that its intensity is inversely proportional to the added oxygen concentration above that of the aerated condition, supporting the Scheme 2 mechanism proposed by Gorman et al.[6] Similar to the derivation to obtain eq 2, the fluorescence response function, $I_{PC}(t)$, defined as the quantum intensity of the delayed PC fluorescence at a time t, can be deduced from (4) and expressed in (5),

$$I_{pc}(t) = \frac{k_f k_3 k_1 [PC][^1\Delta_g]_0}{k_2 k_{pc}[^3\Sigma_g^-]} e^{-2(k_p + k_q[PC])t} \quad (5)$$

where k_f is the radiative decay rate of PC*. Accordingly, the measured emission intensity of PC delayed fluorescence, F_{PC}, an be expressed in eq 6.

$$F_{pc} = \alpha \frac{k_f k_1 k_3 [PC][^1\Delta_g]_0^2}{2(k_p + k_q[PC])k_{pc} k_2 [^3\Sigma_g^-]} \quad (6)$$

Under an identical experimental configuration, i.e., the same α

value and number of photons being absorbed, the ratio of the sensitized PC fluorescence intensity (6) versus the dimol emission intensity (3) can be shown in eq 7

$$\frac{F_{PC}}{F_D} = 2\left(\frac{k_1}{k_2}\right)\left(\frac{k_f}{k_{PC}}\right)\frac{[PC]}{[^3\Sigma_g^-]}\left(\frac{k_{-ac}}{k_D}\right)\left(\frac{k_p}{k_p + k_q[PC]}\right)\left(\frac{k_3}{k_{ac}}\right) \quad (7)$$

We first attempted to resolve the photophysical parameters in eq 7, which can be either experimentally obtained or theoretically estimated. The value of k_f/k_{pc} is equivalent to the quantum yield of PC fluorescence, which has been determined to be 0.72 in CCl_4. For the next step, the value of $k_p/(k_p + k_q[PC])$ can be simply obtained by a Stern−Volmer relationship using $^1\Delta_g \rightarrow {}^3\Sigma_g^-(0,0)$ 1273 nm emission shown in eq 8, where

$$\frac{I_0}{I} = \frac{k_p + k_q[PC]}{k_p} \quad (8)$$

I_0 and I denote the $^1\Delta_g$ 1273 nm emission in CCl_4 and CCl_4 containing PC, respectively. Plotting I_0/I of against the PC concentration, the slope was determined to be 2.44×10^4 M^{-1}. In an identical setup but using a chopped 514 nm excitation pulse (see the Experimental Section for the detailed description), k_p was determined to be 154 s^{-1} ($\tau = 6.5$ ms). As a result, the quenching rate k_q for PC was calculated to be 3.76×10^6 M^{-1} s^{-1} in CCl_4. This measured k_q value is ∼2 orders of magnitude smaller than that of 2.4×10^8 s^{-1} M^{-1} for PC reported by Krasnovsky et al. in $CHCl_3$.[27] To check the validity of our result in CCl_4, we have reinvestigated k_q of PC in $CHCl_3$. Under identical experimental conditions with that in CCl_4, a k_q value of 2.6×10^8 s^{-1} M^{-1} in $CHCl_3$ was determined, which only differs from that obtained by Krasnovsky et al. by ∼10%. Our results also showed that k_q of PC increases drastically upon increasing solvent polarity, especially in protic solvents, indicating that certain types of charge-transfer mechanism may play a role in the quenching process. Studies focusing on the solvent-dependent $^1\Delta_g$ quenching rate for PC will be published elsewhere. k_1/k_2 is simply the equilibrium constant between $^1\Delta_g$ and $PC(T_1)$[6] and is equivalent to $e^{-\Delta E/RT}$ where ΔE is the energy difference between $^1\Delta_g$ and $PC(T_1)$ states, assuming that the change of entropy factor is negligible. To obtain ΔE we have performed a phosphorescence study of PC in a 77 K methyltetrahydrofuran glass and measured the onset of the PC phosphorescence, defined by its first vibronic transition peak, to be near 9200 cm^{-1} (1087 nm). Knowing that $^1\Delta_g$ lies 7855 cm^{-1} above the $^3\Sigma_g^-$ state, k_1/k_2 was then calculated to be 1.51 $\times 10^{-3}$. Finally, it is reasonable to assume that k_3 and k_{ac} are both diffusion-controlled processes and can thus be canceled out in eq 7. Giving the $O_2(^3\Sigma_g^-)$ concentration to be 2.48×10^{-3} M in the aerated CCl_4,[12] eq 7 can be simplified to (9)

$$\frac{F_{PC}}{F_D} = 0.88\left(\frac{k_{-ac}}{k_D}\right)\left(\frac{k_p}{k_p + k_q[PC]}\right)[PC] = 0.88\left(\frac{k_{-ac}}{k_D}\right)\left(\frac{I}{I_0}\right)[PC] \quad (9)$$

Experimentally, using the C_{60} fluorescence intensity as a mutual reference, F_{PC}/F_D, within the experimental error, was found to be linearly proportional to $[I/I_0][PC]$ (see Figure 4) when the PC concentration varied from 1.25×10^{-6} to 1.25×10^{-5} M, consistent with the theoretical approach depicted in eq 9. The slope in Figure 4 was determined to be $(2.3 \pm 0.2) \times 10^9$ M^{-1}. This gives a k_{-ac}/k_D value of $(2.6 \pm 0.3) \times 10^9$. Based on the absorption cross section of O_2 dimol in the high-pressure gas phase, the value of k_D has been theoretically calculated to be 0.67 s^{-1}.[28] On the other hand, in an argon matrix isolated

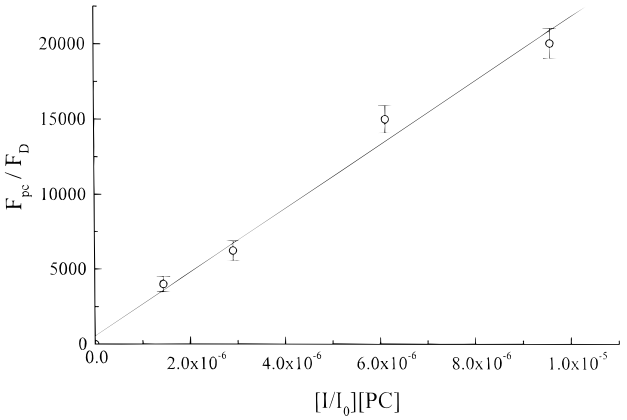

Figure 4. Plot of F_{PC}/F_D versus $[I/I_0][PC]$ by varying the PC concentration from 1.25×10^{-6} to 1.25×10^{-5} M (see the text for the detailed description).

system, the decay rate of the $(^1\Delta_g)_2(0,0) \rightarrow (^3\Sigma_g^-)_2(0,0)$ transition has been measured to be on the average of 10^1 s^{-1} at 4 K.[29a] Assuming that the thermally activated radiationless process is negligible at 4 K, this k_D value is more than 1 order of the magnitude greater than that in the gas phase, indicating that certain geometry perturbation by the solvent cage may play a role which leads to a partially allowed electric−dipole transition. Taking k_D in CCl_4 to be similar to that measured in an argon matrix, a value of $(2.6 \pm 0.3) \times 10^{10}$ M^{-1} s^{-1} was deduced for k_{-ac}. This calculated τ_{-ac} ($=1/k_{-ac}$) of ∼38 ps is about 1 order of magnitude longer than the estimated dissociation rate in the gas phase of a few picoseconds,[28] indicating a possibility that the solvent cage may play a role in restricting the dissociation of the dimol species. However, since the k_{-ac} value was deduced by taking the known k_D in an argon matrix, significant error may be introduced when the k_D value measured in CCl_4 is different from that in argon. For example, the lifetime of $^1O_2$ dimol in neon has been reported to be shorter than that in argon by 2 orders of magnitude (1.2 ms in neon[29b] versus 100 ms in argon[29a]) due to the stronger perturbation. In CCl_4, it is also reasonable to predict that the dimol susceptible to the perturbation is stronger than that in an argon matrix, resulting in a larger k_D. Consequently, k_{-ac} calculated according to eq 9 should increase. Therefore, the deduced k_{-ac} of $(2.6 \pm 0.3) \times 10^{10}$ M^{-1} s^{-1} in this study may be considered as a lower limit for the dimol dissociation rate. Nevertheless, the deduced k_{-ac} value of 2.6×10^{10} s^{-1} is $\gg k_{ac}[^1\Delta_g]$, fulfilling a requirement of the steady-state approximation for the relaxation dynamics of $[(^1\Delta_g)_2]$.

Earlier studies based on C_{60} quenching the triplet state of various organic molecules, in which the lowest triplet-state energies have been known, estimated the lowest triplet-state energy (E_T) of C_{60} in benzene to be 33 kcal/mol ≤ E_T < 42 kcal/mol.[30] Subsequently, an E_T value of 36.3 kcal/mol in benzene has been determined by phosphorescence studies of C_{60} at low temperature.[31,32] Further measurement using a method of photoacoustic calorimetry precisely determined the E_T value to be 36.0 ± 0.6 kcal/mol in toluene.[33] The energy gap between $^1\Sigma_g^+$ and $^3\Sigma_g^-$ states has been measured to be 37.3 kcal/mol in CCl_4 ,[13] the absence of O_2 $^1\Sigma_g^+ \rightarrow {}^3\Sigma_g^-$ (765 nm) emission (see Figure 2c) suggests the upper limit of C_{60} (E_T) to be 37.3 kcal/mol in CCl_4. Further support is given by the study of the $^1\Sigma_g^+ \rightarrow {}^1\Delta_g$ transition using a Fourier transform technique (see the Experimental Section for a detailed description). Figure 5a shows the $^1O_2$ emission in CCl_4 sensitized by PH in the region of 4000−10 000 cm^{-1}. Three vibronic peaks maxima at 1273 (7855 cm^{-1}), 1588 (6297 cm^{-1}), and 1925 nm (5195

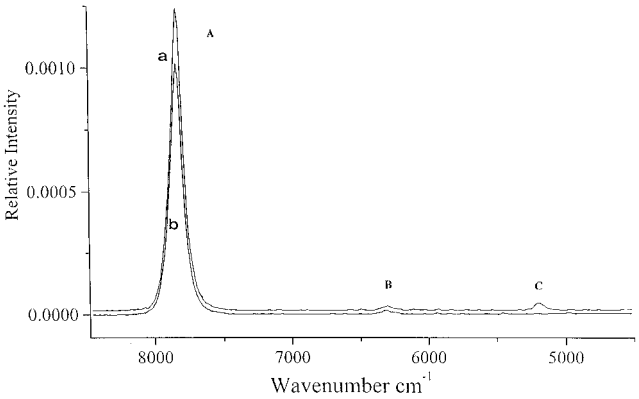

Figure 5. Emission spectrum of O_2 (1.2×10^{-2} M) sensitized by (a) PH (3.14×10^{-4} M) and (b) C_{60} (9.0×10^{-5} M) at 25 °C. Peaks A and B correspond to the $O_2(^1\Delta_g) \rightarrow (^3\Sigma_g^-)$ (0,0) and (0,1) transition, respectively, and peak C to the $O_2(^1\Sigma_g^+) \rightarrow (^1\Delta_g)(0,0)$ transition. The sensitizers were excited by a CW Ar^+ laser (350 nm, 50 mW with a beam diameter of 2.0 mm).

cm^{-1}) were resolved, corresponding to O_2 $^1\Delta_g \rightarrow {}^3\Sigma_g^-(0,0)$, $^1\Delta_g \rightarrow {}^3\Sigma_g^-(0,1)$, and $^1\Sigma_g^+ \rightarrow {}^1\Delta_g(0,0)$ transitions, respectively. In comparison to Figure 5a, Figure 5b shows C_{60}-sensitized $^1O_2$ emission under identical experimental conditions. Although similar O_2 $^1\Delta_g \rightarrow {}^3\Sigma_g^-$ 1273 and 1588 nm emission was observed, after normalizing the 1273 nm vibronic peak, the $^1\Sigma_g^+ \rightarrow {}^3\Sigma_g^-(0,0)$ transition, under our detection limit, was not detected. The result indicates that the production of the $^1\Sigma_g^+$ state through the $(C_{60}(E_T)-{}^3O_2)$ collisional complex may be energetically unfavorable, i.e., $C_{60}(E_T) < 37.3$ kcal/mol in CCl_4. It should be noted that this conclusion made on the basis of a thermodynamic approach may only be qualitative. Other mechanisms incorporating a very small branching ratio for Σ_g^+ versus $^1\Delta_g$ production upon C_{60} sensitization may also be possible to explain the lack of $^1\Sigma_g^+$ emission. The absence of both 765 and 1925 nm emission originating from the $^1\Sigma_g^+$ state further suggests that the energy pooling process $(^1\Delta_g)_2 \rightarrow {}^1\Sigma_g^+ + {}^3\Sigma_g^-$ depicted in Scheme 1 is at least not a major decay pathway. This result is also consistent with the peroxide hypochlorite reaction which produces O_2 in the $^1\Delta_g$ state predominantly, while the $^1\Sigma_g^+$ production is very small and mainly from the energy pooling process, with the $[^1\Sigma_g^+]/[^1\Delta_g]$ being less than 10^{-6}.[34]

Conclusion

In conclusion, we have reported spectroscopic and photophysical studies of ultraweak $^1O_2$ emission in the visible region. The dissociation rate of $^1O_2$ dimol, k_{-ac}, has been estimated to be $(2.6 \pm 0.3) \times 10^{10}$ s^{-1}. Further attempts have to be made to extract the actual k_D value in CCl_4. One possible solution is to apply the mechanism of $O_2(^1\Delta_g)$ dimol sensitized luminescence for certain dyes, in which the decay dynamics should also involve k_{ac} and k_{-ac}. Therefore, both k_{ac} and k_{-ac} can be eliminated when comparing the emission intensity with respect to that of the $O_2(^1\Delta_g)$ dimol to extract the k_D value. Unfortunately, there has been no chemical systems showing evidence to support the $O_2(^1\Delta_g)$ dimol-sensitization mechanism at this stage.[6] Studies focused on this subject are currently in progress.

Acknowledgment. Support from the National Chung-Cheng University and National Science Council (grant NSC85-2113-M-194-005) is gratefully acknowledged.

References and Notes

(1) Schmidt, R. Ber. *Bunsen-Ges. Phys. Chem.* **1992**, *96*, 794.
(2) Schmidt, R.; Bodesheim, M. *Chem. Phys. Lett.* **1993**, *213*, 111.
(3) Schmidt, R.; Bodesheim, M. *J. Phys. Chem.* **1994**, *98*, 2874.
(4) Schmidt, R.; Bodesheim, M. *J. Phys. Chem.* **1995**, 99, 15919.
(5) Krasnovsky, A. A. Jr.; Foote, C. S. *J. Am. Chem. Soc.* **1993**, *115*, 6013..
(6) Gorman, A. A.; Hamblett, I.; Hill, T. J. *J. Am. Chem. Soc.* **1995**, *117*, 10751.
(7) Chou, P. T.; Wei, G. T.; Lin, C. H.; Wei, C. Y.; Chang, C. H. *J. Am. Chem. Soc.* **1996**, *118*, 3031.
(8) Kim, D.; Lee, M.; Suh, Y. D.; Kim, S. K. *J. Am. Chem. Soc.* **1992**, *114*, 4429.
(9) Sun, Y. P.; Wang, P.; Hamilton, N. B. *J. Am. Chem. Soc.* **1993**, *115*, 6378.
(10) Mikhalenko, S. A.; Barkianova, O. L.; Lebedev, L. O.; Lukjanetz, E. A. *Zh. Obsch. Khim. (J. Gen. Chem. USSR)* **1971**, *41*, 2770.
(11) Ajie, H.; Alvarez, M. M.; Anz, S. A.; Beck, R. D.; Diederich, F.; Fostiropoulos, K.; Huffman, D. R.; Kratschmer, W.; Rubin, Y.; Schriver, K. E.; Sensharma, D.; Whetten, R. L. *J. Phys. Chem.* **1990**, *94*, 8630.
(12) Battino, R.; Rettich, T. R.; Tominaga, T. *J. Phys. Chem. Ref. Data* **1983**, *12(2)*, 163.
(13) Chou, P. T.; Frei, H. *Chem. Phys. Lett.* **1985**, *122*, 87.
(14) Chou, P. T.; Frei, H. *J. Chem. Phys.* **1987**, *87(7)*, 3843.
(15) Schmidt, R.; Brauer, H. D. *J. Am. Chem. Soc.* **1987**, *109*, 6976.
(16) Chou, P. T.; Wei, C. Y.; Chang, C. P.; Kuo, M. S. *J. Phys. Chem.* **1995**, *99*, 11994.
(17) Sension, R. J.; Phillips, C. M.; Szarka, A. Z.; Romanow, W. J.; McGhie, A. R.; McClauley, J. P., Jr.; Smith, A. B.; Hochstrasser, R. M. *J. Phys. Chem.* **1991**, *95*, 6075.
(18) Ebbsen, T. W.; Tanigaki, K.; Kuroshima, S. *Chem. Phys. Lett.* **1991**, *181*, 501.
(19) Wasielewski, M. R.; O'Neil, M. P.; Lykke, K. R.; Pellin, M. J.; Gruen, D. M. *J. Am. Chem. Soc.* **1991**, *113*, 2774.
(20) *CRC Handbook of Chemistry and Physics*, 68th ed.; CRC Press: Boca Raton, FL; p E−371.
(21) Oliveros, E.; Suardi-Murasecco, P.; Aminian-Saghafi, T.; Braun, A. M.; Hansen, H.-J. *Helv. Chim. Acta* **1991**, *74*, 79.
(22) Kransovsky, Jr. A. A. *Photochem. Photobiol.* **1979**, *29*, 29.
(23) Salokhiddinov, K. I.; Dzhagarov, D. M.; Byteva, I. M.; Guinovich, G. P. *Chem. Phys. Lett.* **1980**, *76*, 85.
(24) Salokhiddnov, K. I.; Dzhagarov, D. M.; Byteva, I. M.; Gurinovich, G. P. *Chem. Phys. Lett.* **1980**, *76*, 85.
(25) Chou, P. T.; Frei, H. *Chem. Phys. Lett.* **1985**, *122*, 87.
(26) Ogryzlo, E. A.; Pearson, A. E. *J. Phys. Chem.* **1968**, *72*, 2913.
(27) Krasnovsky, A. A.; Rodgers, M. A. J.; Galpern, M. G.; Rither, B.; Kenny, M. E.; Lukjanetz, E. A. *Photochem. Photobiol.* **1992**, *55*, 691.
(28) Arnold, S. J.; Kubo, M.; Ogryzlo, E. A. *Adv. Chem. Ser.* **1968**, 77, 133.
(29) (a) Becher, A. C.; Schurath, U.; Dubost, H.; Galaup, J. P. *Chem. Phys.* **1988**, *125*, 321. (b) Goodman, J.; Brus, L. E. *J. Chem. Phys.* **1977**, *67*, 4408.
(30) Arbogast, J. W.; Darmanyan, A. P.; Foote, C. F.; Rubin, Y.; Diederich, F. N.; Alvarez, M. M.; Anz, S. J.; Whetten, R. L. *J. Phys. Chem.* **1991**, *95*, 11.
(31) Zeng, Y.; Biozok, L.; Linschitz, H. *J. Phys. Chem.* **1992**, *96*, 5237.
(32) Sibley, S. P.; Argentine, S. M.; Francis, A. H. *Chem. Phys. Lett.* **1992**, *188*, 187.
(33) Hung, R. R.; Grabowski, J. J. *J. Phys. Chem.* **1991**, *95*, 6073.
(34) Khan, A. U.; Kasha, M. *J. Am. Chem. Soc.* **1970**, *92*, 3293.